

See discussions, stats, and author profiles for this publication at: <https://www.researchgate.net/publication/263961969>

Highlighting a Cooling Regime in Liquids under Submillimeter Flows

ARTICLE *in* JOURNAL OF PHYSICAL CHEMISTRY LETTERS · JUNE 2013

Impact Factor: 7.46 · DOI: 10.1021/jz400673d

CITATION

1

READS

20

3 AUTHORS, INCLUDING:



[Patrice Bouchet](#)

Atomic Energy and Alternative Energies Com...

257 PUBLICATIONS 1,645 CITATIONS

SEE PROFILE



[Laurence Noirez](#)

French National Centre for Scientific Research

121 PUBLICATIONS 1,236 CITATIONS

SEE PROFILE

Highlighting a Cooling Regime in Liquids under Submillimeter Flows

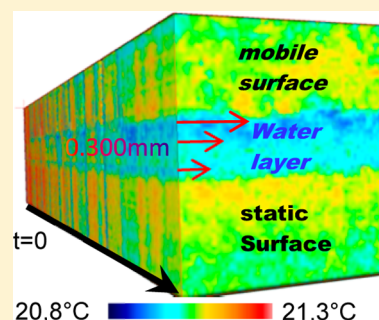
Patrick Baroni,[†] Patrice Bouchet,[‡] and Laurence Noirez^{*,†}

[†]Laboratoire Léon Brillouin (CEA-CNRS), Ce-Saclay, 91191 Gif-sur-Yvette Cédex, France

[‡]UMR7158 DSM/IRFU Service d'Astrophysique, Ce-Saclay, 91191 Gif-sur-Yvette Cédex, France

ABSTRACT: The shear flow of ordinary liquids is for the first time observed at the submillimeter scale by thermal imaging. We report on microinfrared experiments, showing that liquids as important as water flowing on wetting surfaces produce cooling, while the academic view would foresee heating production. This apparent counter-intuitive cooling effect shows that the increase of the internal energy due to the flow can result in different shapes, including a cooling process, before reaching the conventional heating regime at higher shear rates. This unknown property might be interpreted as a transient stretching state of the liquid. Shearing liquids might be a promising alternative compared to conventional endothermic processes (gas expansion or vaporization of a liquid, the Peltier effect, and so forth).

SECTION: Energy Conversion and Storage; Energy and Charge Transport



Despite considerable experimental and theoretical efforts, we still hardly understand, poorly control, and fully ignore the thermal exchanges that take place in liquids under flow. The flow in simple liquids is ideally depicted by a displacement by molecular friction from layer to layer, producing a shear gradient characterized by a shear rate $\dot{\gamma}$ defined as the ratio of the thickness to the shear velocity v , $\dot{\gamma} = v/e$ (Figure 1a). The friction mechanism at the origin of the viscosity is theoretically supposed to generate heating. This assumption, proposed by Eyring in years 1931–1945,¹ is commonly adopted in scientific and industrial communities and is verified in conventional flow measurements.^{2,3} The study of flow at the submillimeter scale assumes nowadays a significant development because of the versatile applications (nozzles, diffusers, pumps, mixers, pipes, heat transfer) that are of interest in various sectors (medical displays, chemical analysis, biotechnology).

We report here on the first thermal imaging of flows at the submillimeter scale. This pioneering approach is carried out by infrared absorption in real time. Recent instrumental advances enable nowadays the detection of thermal variations as small as 0.01 °C and with a time resolution of about 0.03s. We highlight the pertinence of this new spectral method in fluids by revealing for the first time that the mechanical energy injected by shearing can produce not only a heating but also, in particular conditions, a very counterintuitive effect, a cooling regime. The shear-induced cooling is observed on various liquids (water, polymer melts, glycerol) using low shear rates and high wetting substrates. This regime might appear as a prior regime before the conventional viscous heating observed at higher shear rates, meaning that the increase of the internal energy due to the mechanical shear can result in a cooling process before the heating regime. In this Letter, we particularly examine the phenomenon of cooling produced by liquid water at low shear rate.

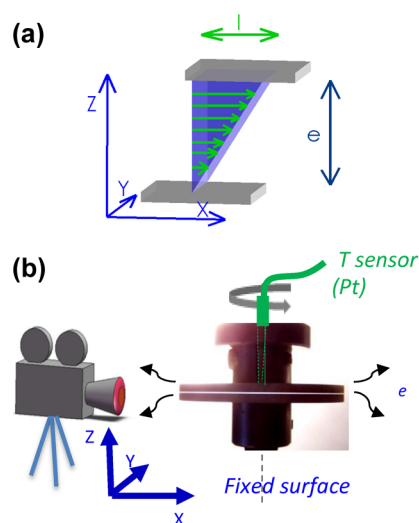


Figure 1. (1) Simple shear flow geometry. The shear rate $\dot{\gamma}$ is defined as the ratio of the thickness to the shear velocity v , $\dot{\gamma} = (\partial v / \partial z) / e = v / e$. (b) Setup: The liquid is sheared between two coaxial alumina disks (of 50 mm diameter separated in the present photograph by 0.100 mm), one of which is driven in a uniform rotational movement and the other fixed. The IR camera is positioned so as to observe the flow in the (velocity (Ox), velocity gradient (Oz)) plane. The shear rate $\dot{\gamma}$ is defined from the velocity at the edges of the disks. The upper disk is equipped with a Pt sensor placed in the middle of the cylinder that surmounts the disk. The sensor is in contact with the upper surface of the disk.

Received: March 27, 2013

Accepted: May 24, 2013

Microthermal Imaging. The thermal mapping is based on the emissivity measurement. Liquids and water in particular present high emissivity coefficients (0.98 for liquid water), fulfilling the conditions to apply the Stefan–Boltzmann law.⁴ This law establishes that a medium radiates all the more when its temperature is high. The heat transfer by radiation can be expressed as $E = e_m \cdot \sigma \cdot A(T^4 - T_c^4)$, where E is the radiated energy, e_m the emissivity, A the radiating area, T the temperature of the sample, and T_c the temperature of the surroundings. σ is the Stefan's constant. A high-performance 320×240 pixels B400 FLIR infrared 2D detector equipped with a close-up lens giving a spatial resolution of $25 \mu\text{m}$ in a $8 \times 6 \text{ mm}^2$ working area is placed at about 50 mm from the free surface of the liquid filling the gap between two wetting substrates made of alumina.^{5,6} The frame rate is 30 Hz. The resolution ellipsoid enables to probe a $\pm 0.15 \text{ mm}$ depth of field. The spectral range goes from 7.5 up to $13 \mu\text{m}$, and the relative temperature accuracy is $\pm 0.025^\circ\text{C}$. The files are renormalized by the thermal measurement recorded at rest (before applying the shear stress). Simultaneously, a conventional Pt sensor records the temperature by contact with the outer side of one surface (Figure 1b).

The shear flow conditions (Figure 1a) are reproduced using two coaxial parallel disks (Figure 1b) (plane–plane geometry). The upper surface rotates, whereas the inferior one is static and coupled to a force sensor. The steady-state shear motion is obtained by a constant rotation of one surface with respect to the other. The experiments are carried out using total wetting boundary conditions between the disk surface and the liquid (total wetting is here obtained using high-density alumina^{5,6}). The high affinity of the liquid to the substrate lowers its propensity to slip on the surface.⁷ The samples are stored at room temperature, and an equilibrium time of at least 30 min is observed prior to the experiment. The thermal maps are recorded at absolute temperature without external thermal input.

Measuring a Shear-Induced Cooling during Water Flow. We first report here on experiments performed on liquid water (similar experiments have been carried out with glycerol and polymers such as polybutadiene measured at about 100°C above the glass transition temperature). The liquid water fills the gap between the two high wetting substrates (Figure 1b). The thermal mapping observation is carried out in the (yOz) plane corresponding to the (velocity, velocity gradient) plane. Low shear rates $\dot{\gamma}$ are applied to keep the conditions of a laminar regime. A coupling with molecular relaxation time τ ($\dot{\gamma}\tau \ll 1$) is irrelevant for liquid water.

The infrared absorption imaging of the thermal emission produced by a layer of the liquid water sheared on wetting substrates is shown in Figure 2a. The high wettability of the substrate favors the anchoring (the contact angle $\theta = 0$ indicates a total wetting of the water). A cooling process is observed in the sheared liquid and is measurable as soon as $\dot{\gamma} \geq 2 \text{ s}^{-1}$.

At higher shear rates, the cooling is more pronounced. Figure 2b shows the evolution of the temperature profile within the gap upon applying a shear rate of $\dot{\gamma} = 20 \text{ s}^{-1}$. At rest, water and the substrates are at the same temperature (Figure 2b and c). At the onset of the shear flow, the cooling is first rapid and then slows down to a stationary state following a typical relaxation law of type $T = (T_0 - T_\infty) \cdot \exp(-(t/\tau_0)^\alpha) + T_\infty$, with $\tau_0 = 70 \text{ s}$ in the middle of the liquid and $\tau_0 = 570 \text{ s}$ in the substrate for $T_0 = 21.25 \pm 0.05^\circ\text{C}$; $T_\infty = 20.5 \pm 0.3$ and $\alpha = 0.25$ in both cases (inset of Figure 2b). This law is rather qualitative and aims at

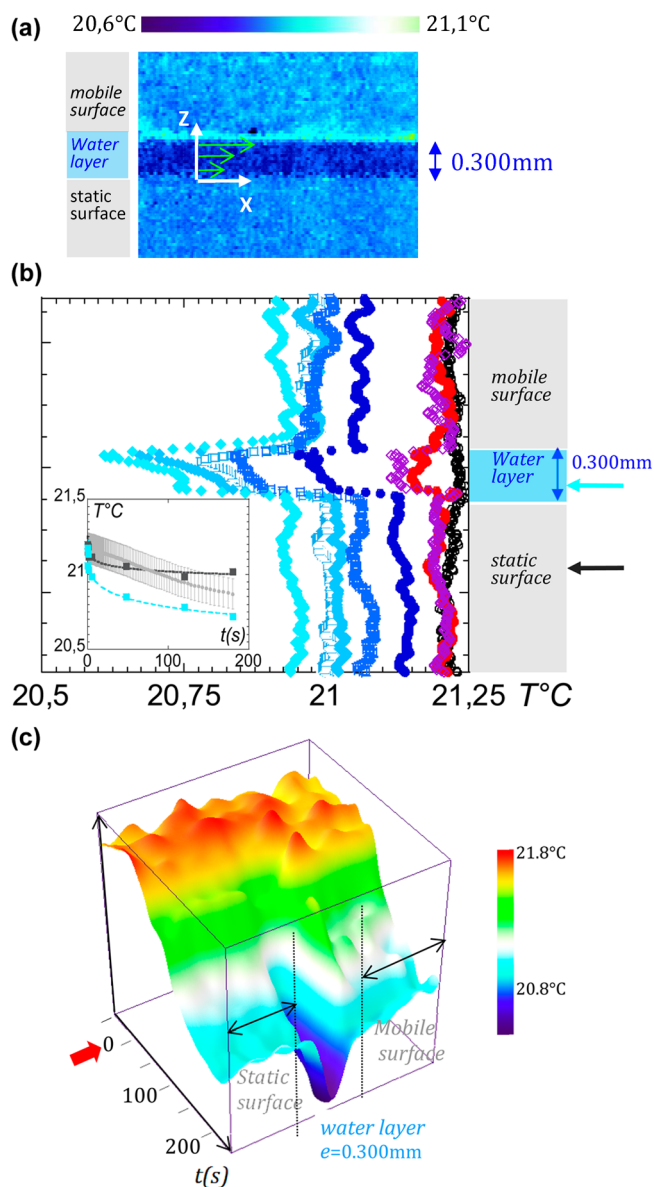


Figure 2. (a) 2D thermal mapping (snapshot) showing cooling of around 0.25°C of the water layer sheared at 2 s^{-1} (0.6 mm/s) between wetting surfaces. The gap thickness is 0.300 mm . (b) Time evolution of the temperature profile in a 0.300 mm water gap (in light blue) sheared at 20 s^{-1} at room temperature ($T_0 = 21.25^\circ\text{C}$) on wetting substrates (gray areas): red \bullet , 0.4 s ; purple \diamond , 1.2 s ; dark blue \bullet , 4.8 s ; light blue \square , 48 s ; aqua \square , 133 s ; light blue \diamond , 120 s ; aqua \diamond , 180 s . The inset presents the temperature evolution in the liquid (light blue arrow and light blue squares) and on the static substrate (dark gray arrow and squares), and the gray points (with large error bars, $\pm 0.1^\circ\text{C}$) correspond to the indirect measurement with the Pt sensor. (c) Time–temperature evolution of a water layer between wetting surfaces from the quiescent state to the application of a constant shear stress at a time $t_0 = 0$ indicated by the red arrow ($\dot{\gamma} = 2 \text{ s}^{-1}$, $e = 0.300 \text{ mm}$; gathering of 650 pictures). The orange area corresponds to the quiescent state (recorded over 40 s).

showing that the cooling invades the whole gap and is transferred to the substrates. Because the depth field of the IR camera is limited at about 0.4 mm from the external surface, the inner cooling is inaccessible. A Pt sensor has been installed in contact at the center of the outside of the upper fixture (Figure 1b). A similar temperature decrease is observed, confirming

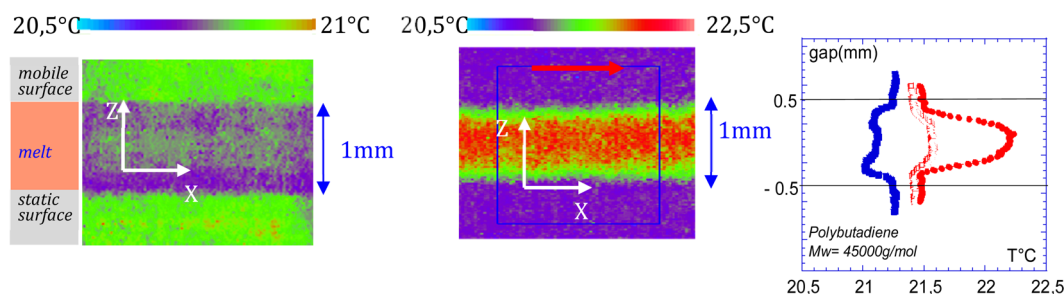


Figure 3. 2D thermal mapping obtained by shearing a polybutadiene melt at room temperature, that is, at 100 °C above the glass transition ($M_w = 45000$ g/mol, 1 mm gap thickness). (left) Low shear rate, $\dot{\gamma} = 1$ s $^{-1}$. The liquid becomes cooler under flow than the fixtures (in green). (middle) High shear rates $\dot{\gamma} = 100$ s $^{-1}$. The melt becomes warmer than the surfaces (in purple). (right) Vertical section showing the temperature profile along the velocity gradient at $\dot{\gamma} = 1$ s $^{-1}$ (blue ■), 20 s $^{-1}$ (red □), 100 s $^{-1}$ (red ●).

that the cooling is not an interfacial mechanism but originates from the whole volume (inset Figure 2b). A cooling by evaporation process is ruled out. A large amount of literature, mostly empirical, enables one to calculate the evaporation rate from a free surface of water.⁸ At room temperature, this rate is on the order of 10^{-5} kg/m 2 ·s.⁹ In the present geometry, the only free surface is the disk circumference. It offers a maximum evaporation rate of 0.5×10^{-6} g/s, which corresponds to 0.12 mm 3 during typical acquisition time ($t = 250$ s), that is, consuming 0.018% of the initial volume. We calculate now the rate necessary to interpret the cooling as resulting from an evaporation effect. On the basis of the heat capacity of the substrate (0.9 J/g·°C) and that of the water (4.18 J/g·°C at atmospheric pressure), the energy loss necessary to decrease the temperature of both substrates (two disks of 35 g) and of a liquid layer (0.590 g) by 0.5 °C is at least of 33 J. The 33 J represents an evaporation rate of 2.5% of the initial water volume. It is compatible with neither the empirical calculation (0.018%) nor the observation. No water loss is perceptible even during much longer times (>1000 s) during which the liquid front is stable within ± 0.15 mm; otherwise, it would have moved out of the narrow camera depth field. In the absence of shear flow, no thermal variation is recorded (Figure 2c), in agreement with a negligible evaporation (an evaporation of 0.018% of the volume should produce a temperature decrease of 0.005 °C, which is negligible and below the accuracy).

Measuring a Shear-Induced Cooling during Polymer Melt Flow. Finally, to rule out definitively the evaporation question, it is important to emphasize that a similar cooling is observable on liquids that do not exhibit vapor tension (polybutadiene) or have a very weak vapor tension (glycol, triethyleneglycol). The low shear rate thermal mapping produced by a polybutadiene melt is illustrated on Figure 3, left. This melt has the consistency of motor oil. At higher shear rates ($\dot{\gamma} > 20$ s $^{-1}$), the cooling (Figure 3, left) is converted in a heating process, as illustrated in Figure 3, middle. From low to high shear rate, the thermal profile exhibits several thermal shear banding that are likely to be related to the so called rheological or birefringent shear banding. The experiment has not been carried out with water because of the high shear rates needed (creating an unstable/mobile interface).

In summary, a so far unknown endothermic process has been identified at the submillimeter scale by shearing liquids on wetting substrates. Appearing at low shear rates, the shear-induced cooling might appear as a prior regime before the “classical” viscous heating process.^{2,3} The experimental conditions and the short time scales considered rule out main artifacts such as the evaporation or the vaporization processes

in the case of liquid water and the observation of a cooling process in low viscous polymer melts (Figure 3, left). The cooling is generated at low shear rates (on the order of s $^{-1}$) excluding a flow coupling to the individual molecular dynamic (the relaxation times of the water molecule and of the polymer are on the order of ps and of 10^{-3} s, respectively¹⁰) but support collective long-range intermolecular correlations.

Because of the intermolecular interactions, liquids are to some extent compressible and correlatively “stretchable”. This property requires the solicitation of no-zero shear elasticity. Recent independent results^{11–17} indicate indeed that liquids are not fully viscous but exhibit an almost static shear elasticity of several Pascals^{11–16} when they are tested at the submillimeter scale with a low-amplitude oscillatory shear stress (Figure 4

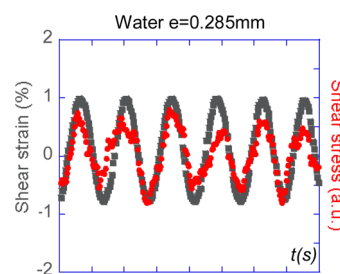


Figure 4. Water response displayed at room temperature to a low-frequency oscillatory shear wave. Input sin strain wave (gray ■) and output shear stress (red ●) wave are close in phase, indicating an instantaneous response, that is, a solid-like behavior (data points from ref 8) (strain amplitude: $\gamma_0 = 3\%$; frequency $\omega = 5$ rad/s; sample thickness $e = 0.285$ mm).

illustrates the elastic (in-phase) response of water).¹⁶ We suggest that the internal energy bought by the flow is used to produce a weakly stretched state. The “loss” of thermal energy (cooling) might be compensated for by the increase of the internal energy required to stretch and should relax via an energy release once the shear flow is stopped. Figure 5, displaying the evolution of the temperature upon relaxation, shows indeed that the temperature is indeed globally elevated once the flow has stopped. This unload of energy by stopping the shear flow correlatively evidences that energy was stored during flow. This mechanism supposes a high degree of intermolecular connectivity. A similar assumption is made to interpret negative-pressure experiments and is also emphasized in several theoretical approaches of the liquid state^{18–21} or in simulations at extreme shear rates.²² Under shear flow, the intermolecular interactions might be under tension similarly as

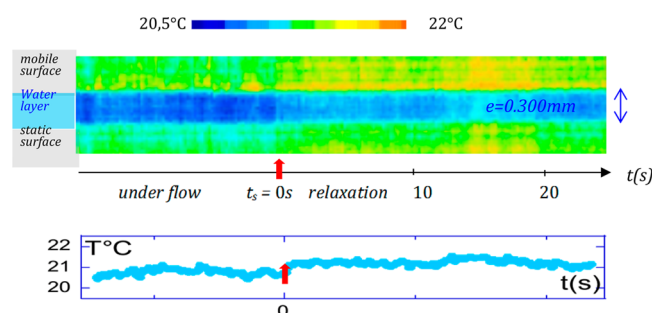


Figure 5. Time–temperature evolution of a 60 μm width snapshot of the gap recorded every 0.04 s (gathering about 800 thermal mapping pictures). The 0.300 mm water layer thickness is submitted to a steady-state shear rate of 20 s^{-1} before the flow stops. The red arrow indicates the instant at which the flow is stopped ($t_s = 0$ s). The average temperature under shear flow is 20.78 ± 0.141 $^{\circ}\text{C}$, while during relaxation, it reaches 21.23 ± 0.136 $^{\circ}\text{C}$.

in solids²³ or in negative-pressure experiments^{24,25} but to a much smaller extent. The (shear)-mechanical tension can be exercised as long as the liquid resists pointing out the central role of the interaction to the substrate (anchoring) for the transmission of the shear stress. The present description focuses on how the energy flows in or out of the liquid and does not treat the total energy balance requiring energy conversation. It aims at showing that the increase of the internal energy due to the flow can result in different shapes, not only in a heating but also in a cooling process, before reaching the heating regime at higher shear rates. Both cooling and heating regimes exhibit thermal shear banding pointing out the complexity and the inhomogeneity of the flow even at the lowest shear rates. The cooling regime has certainly profound implication for physics and biology (water) that goes beyond the present purpose. It might also be explored as a promising alternative technology for cold production with several advantages, easy to use, requiring no fuel (recycled fluid), and chemically, mechanically, and thermally stable.²⁶

AUTHOR INFORMATION

Corresponding Author

*E-mail: laurence.noirez@cea.fr. Tel: 33 1 69 08 63 00.

Notes

The authors declare no competing financial interest.

ACKNOWLEDGMENTS

We would like to thank F. Volino and T. Midavaine for their fruitful comments and advice.

REFERENCES

- (1) Milne-Thomson, L. M. *Theoretical hydrodynamics*, 3rd ed.; Macmillan: London, 1995.
- (2) Morini, G. L. Viscous Heating in Liquid Flows in Micro-Channels. *Int. J. Heat Mass Transfer* **2005**, *48*, 3637–3647.
- (3) Morini, G. L. Single-Phase Convective Heat Transfer in Microchannels: A Review of Experimental Results. *Int. J. Thermal Sci.* **2004**, *43*, 631–651.
- (4) Boltzmann, L. Ableitung des Stefan'schen Gesetzes, betreffend die Abhängigkeit der Wärmestrahlung von der Temperatur aus der Electromagnetischen Lichttheorie. *Ann. Phys. Chem.* **1884**, *22S*, 291–294.
- (5) Mendil, H.; Baroni, P.; Noirez, L. Solid-Like Rheological Response of Non-Entangled Polymers in the Molten State. *Eur. Phys. J. E* **2006**, *19*, 77–85.

- (6) Baroni, P.; Mendil, H.; Noirez, L. French Patent 05 10988 (PCT), 2005.
- (7) Blake, T. D. Slip between a Liquid and a Solid: D.M. Tolstoi's (1952) Theory Reconsidered. *Colloids Surf.* **1990**, *47*, 135–145.
- (8) Boelter, L. M. K.; Gordon, H. S.; Griffin, J. R. Free Evaporation into Air of Water from Free Horizontal Quiet Surface. *Ind. Eng. Chem.* **1946**, *38*, 596–600.
- (9) Sartori, E. A Critical Review Employed for the Calculation of the Evaporation Rate from Free Surfaces. *Solar Energy* **2000**, *68*, 77–89.
- (10) Noirez, L.; Mendil-Jakani, H.; Baroni, P. New Light on Old Wisdoms on Molten Polymers. *Macromol. Rapid Commun.* **2009**, *30*, 1709–1714.
- (11) Badmaev, B. B.; Bazaron, U. B.; Derjaguin, B. V.; Budaev, O. R. Measurement of the Shear Elasticity of Polymethylsiloxane Liquids. *Physica B* **1983**, *122*, 241–245.
- (12) Derjaguin, B. V.; Bazaron, U. B.; Lamazhapova, Kh. D.; Tsidypov, B. D. Shear Elasticity of Low-Viscosity Liquids at Low Frequencies. *Phys. Rev. A* **1990**, *42*, 2255–2258.
- (13) Noirez, L.; Baroni, P.; Mendil-Jakani, H. The Missing Parameter in Rheology: Hidden Solid-Like Correlations in Liquid Polymers and Glass Formers. *Polym. Int.* **2009**, *58*, 962–968.
- (14) Noirez, L.; Baroni, P. Revealing the Solid-Like Nature of Glycerol at Ambient Temperature. *J. Mol. Struct.* **2010**, *972*, 16–21.
- (15) Noirez, L.; Mendil-Jakani, H.; Baroni, P. Identification of Finite Shear-Elasticity in the Liquid State of Molecular (OTP) and Polymeric Glass Formers (PBuA). *Philos. Mag.* **2011**, *91*, 1977–1986.
- (16) Noirez, L.; Baroni, P. Identification of a Low Frequency Elastic Behaviour in Liquid Water. *J. Phys.: Condens. Matter* **2012**, *24*, 372101–372107.
- (17) Collin, D.; Martinoty, P. Dynamic Macroscopic Heterogeneities in a Flexible Linear Polymer Melt. *Physica A* **2002**, *320*, 235–248.
- (18) Granato, A. V. Mechanical Properties of Simple Condensed Matter. *Mater. Sci. Eng., A* **2009**, *521*, 6–11.
- (19) Dyre, J. C. Solidity of Viscous Liquids. *Phys. Rev. E* **1999**, *59*, 2458–2459.
- (20) Dyre, J. C. Solidity of Viscous Liquids. *Phys. Rev. E* **2006**, *74*, 21502–21509.
- (21) Volino, F. Théorie Visco-Élastique Non-Extensive. *Ann. Phys.* **1997**, *22*, 7–231.
- (22) Tseng, H.-C.; Wu, J.-S.; Chang, R.-Y. Shear Thinning and Shear Dilatancy of n-Liquid Hexadecane. *J. Chem. Phys.* **2008**, *129*, 14502–20.
- (23) Towle, L. C. Empirical Relationship between Shear Strength, Pressure and Temperature. *Appl. Phys. Lett.* **1967**, *10*, 317–320.
- (24) Debenedetti, P. G. *Metastable Liquids: Concepts and Principles*; Princeton University Press: Princeton, NJ, 1996.
- (25) Caupin, F.; Arvengas, A. A.; Davitt, A. K.; El Mekki Azouzi, M.; Shmulovich, K. I.; Ramboz, C.; Sessoms, D. A.; Stroock, A. D. Exploring Water and Other Liquids at Negative Pressure. *J. Phys.: Condens. Matter* **2012**, *24*, 284110–284117.
- (26) Baroni, P.; Noirez, L.; Bouchet, P. French Patent n°FR1255629, 2012.